Spectrochimica Acta Part A: Molecular and Biomolecular Spectroscopy 307 (2024) 123629

Contents lists available at ScienceDirect

Spectrochimica Acta Part A:
Molecular and Biomolecular Spectroscopy

journal homepage: www.journals.elsevier.com/spectrochimica-acta-part-a-molecular-and-biomolecular-spectroscopy

Membrane-specific and calcium-dependent binding of the *Arabidopsis* C2 domain protein CaLB revealed by ATR-FTIR spectroscopy

Shane Maguire [a], Christian Scheibe [a], Terese Eisgruber [a], Niccolò Mosesso [b], Erika Isono [b], Karin Hauser [a,*]

[a] Department of Chemistry, University of Konstanz, 78457 Konstanz, Germany
[b] Department of Biology, University of Konstanz, 78457 Konstanz, Germany

HIGHLIGHTS

- Membrane binding of the protein CaLB is analysed by ATR-FTIR spectroscopy.
- Use of biomimetic membranes reveal increased affinity to PI(3)P lipids.
- Binding affinity is calcium-dependent.
- Higher calcium concentration increases binding affinity.
- Only minor conformational changes occur upon binding.

GRAPHICAL ABSTRACT

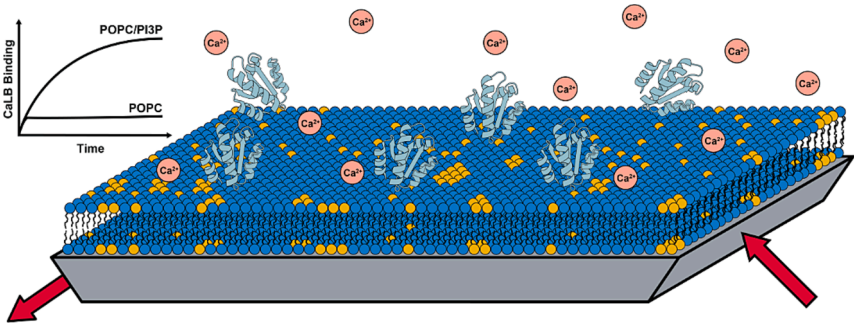

ARTICLE INFO

Keywords:
ATR-FTIR spectroscopy
Protein-membrane binding
Biomimetic membrane
Lipid specificity
Calcium-dependent binding

ABSTRACT

C2 domain-containing proteins bind to cellular membranes and mediate diverse cellular processes. Although many of these membrane-interacting proteins have been identified, the molecular mechanisms of protein-membrane interactions and conformational dynamics are often poorly understood and remain to be investigated with appropriate methods. Here, we used attenuated total reflection Fourier-transform infrared (ATR-FTIR) spectroscopy and biomimetic membrane systems to analyse CalB, a yet uncharacterized *Arabidopsis* C2 domain protein. We studied membrane binding, lipid specificity and calcium dependency with solid-supported lipid membranes (SSLB) and small unilamellar lipid vesicles (SUVs). Membranes were composed of pure POPC lipids or of POPC/PI(3)P lipid mixtures. A significantly increased protein binding affinity was observed with membranes containing 1% PI(3)P indicating the high binding specificity of CaLB for PI(3)P. Furthermore, membrane binding occurs in a calcium-dependent manner with a higher calcium concentration increasing the binding of CaLB to the POPC/PI(3)P membrane. Secondary structure analysis of IR-spectra reveals that only minor conformational changes take place upon binding with a slight increase in the helical and disordered regions of CaLB.

* Corresponding author at: Department of Chemistry, University of Konstanz, 78457 Konstanz, Germany.
E-mail address: karin.hauser@uni-konstanz.de (K. Hauser).

https://doi.org/10.1016/j.saa.2023.123629
Received 16 March 2023; Received in revised form 2 November 2023; Accepted 6 November 2023
Available online 8 November 2023

1. Introduction

C2 domains are membrane-binding modules which are found in eukaryotic proteins [1–3]. A variety of C2 domain proteins have been identified since their discovery, most of them are involved in membrane trafficking and in signal transduction. C2 domains are structurally defined as all-beta protein members of the C2 domain superfamily of Ca^{2+}/lipid-binding domains (CaLB) [4]. C2 domains share a common overall fold consisting of a β-sandwich core connected by flexible loops and helices. These domains were reported to act as Ca^{2+}-activated membrane-targeting motifs, thus they bind to calcium and interact with membrane lipids. However, the targeting process at the plasma membrane is not well understood and the binding affinities for calcium or for specific membrane lipids can vary among different C2 domain proteins. Phosphoinositides are involved in various signaling pathways and in the regulation of membrane traffic [5]. They have been reported as lipid targets for several C2 domains [6–9]. For the characterization of a C2 domain protein with respect to its membrane interactions and the identification of specific lipids to which the C2 domain preferentially binds, *in vitro* studies with molecular resolution are desirable.

Infrared (IR) spectroscopy is a well-suited method to study protein-membrane interactions as well as conformational changes in protein structures [10–16]. IR spectra recorded in a time-resolved manner during the protein-membrane binding process reveal the molecular interactions of the protein with the lipid membrane because characteristic vibrational modes of the functional groups are resolved. The binding specificity of the C2 domain to certain lipids can be investigated and quantified in a systematic way by use of biomimetic membrane models. Biomimetic membranes provide appropriate representations of cell membranes with controllable membrane properties and without the complexity of the living cell. Lipid vesicles are evident mimics for cell membranes, but also solid-supported lipid bilayers (SSLB) are widely used to investigate protein-membrane interactions [17–24]. Biomimetic membranes allow for the preparation of selected lipid compositions and thus to systematically analyse specific lipid interactions [25].

In this study, ATR-FTIR spectroscopy was applied to gain insights into the membrane binding process of the yet uncharacterized C2 domain protein CaLB from *Arabidopsis thaliana*. Calcium dependency, lipid specificity and potential conformational changes occurring upon binding were in the focus of our analyses. Fig. 1 illustrates our experimental approach that allows for the preparation of solid-supported lipid bilayers or lipid vesicles using specific lipid compositions, an easy exchange of protein or buffer solutions with defined calcium concentrations, and the detection of protein conformational changes upon binding to the membrane. IR spectra of protein-membrane binding were recorded in a time-dependent manner and at different calcium concentrations. The effect of membrane curvature was analysed by comparing SSLB and SUV membrane models. The specificity of CaLB binding to the inositol phospholipid PI(3)P was investigated by quantifying the change in protein binding affinity with and without PI(3)P present in the membrane.

2. Experimental section

2.1. Protein expression and purification

CaLB-6xHis was cloned (AT4G34150) into the pET21a vector (Merck Millipore) and expressed in Rosetta (DE3) *E.Coli* strain. The expression of recombinant proteins was induced with 0.4 mM IPTG at 18 °C overnight. The bacterial pellet was resuspended in Buffer A (50 mM Tris (pH 7.4), 100 mM NaCl, 10% glycerol) supplemented with 10 mM imidazole, 0.2% Triton X-100 and cOmplete™, EDTA-free Protease Inhibitor Cocktail (Roche). After sonification, the crude extracts were centrifuged at 16,000xg for 10 min at 4 °C and the supernatant was incubated with TALON metal affinity resin (Takara Bio) for 2 h at 4 °C. The resin was washed extensively with Buffer A supplemented with 10 mM imidazole and 0.2% Triton X-100 and the His-tagged proteins were eluted with Buffer A supplemented with 500 mM imidazole. For the removal of imidazole and Triton X-100, the eluate was subsequently subjected to buffer exchange using PD Spintrap™ G-25 columns (Cytiva).

2.2. Membrane preparation and experimental procedure

POPC (1-palmitoyl-2-oleoyl-*sn*-glycero-3-phosphocholine) and PI(3)P (1,2-dioleoyl-*sn*-glycero-3-phospho-(1′-myo-inositol-3′-phosphate) were purchased from Avanti Polar Lipids, USA. Both, pure POPC and POPC/PI(3)P membranes were prepared. For POPC/PI(3)P (99:1) membrane composition, POPC was dissolved in chloroform at 25 mg/ml and PI(3)P was dissolved at 0.5 mg/ml. 198 µl of POPC and 100 µl of PI(3)P were mixed and gently dried in a glass vial before being put under a vacuum for 120 min. After the removal of chloroform, the lipids were resuspended in 1 ml Buffer A and incubated at room temperature for 30 min. The resuspended solution was sonicated with a tip sonicator (Hielscher Ultrasound Technology, Germany) followed by extrusion using an extruder with a 30 nm polycarbonate membrane from Avanti Polar to produce small unilamellar lipid vesicles (SUVs).

The internal reflection element (IRE) of the ATR cell, a silicon crystal, was polished using a smooth cloth and a 0.1 µm diamond polishing paste. For the SSLB studies, the IRE was pre-treated using H_2SO_4 (95%) for 10 min followed by rinsing with water under a stream of nitrogen gas. This activation procedure was repeated three times and generates a hydrophilic surface of the IRE for vesicle spreading and lipid bilayer formation. 30 µl of the unilamellar vesicle solution were added to the pre-treated IRE and the formation of the lipid bilayer was monitored spectroscopically for 40 min at 25 °C [19,23]. To remove lipids from the supernatant, the IRE was rinsed afterwards for 20 min using Buffer A containing the Ca^{2+} concentration of interest. CaLB protein was dissolved at 0.1 mg/ml concentration in the same buffer/Ca^{2+} solution as for the rinse step. 65 µl were added to the SSLB and spectra were recorded for 120 min. Afterwards, the ATR crystal was rinsed with the buffer/Ca^{2+} solution for further 40 min to remove the protein from the supernatant. A spectrum was recorded afterwards to confirm the binding of the protein to the membrane. For the vesicle studies, the IRE was not activated with H_2SO_4. 30 µl of the unilamellar vesicle solution were

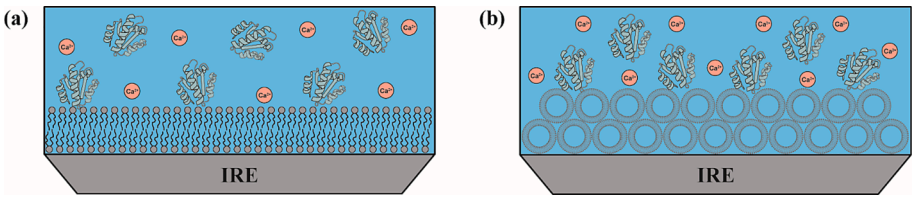

Fig. 1. Scheme of the ATR-FTIR experimental set-up to analyse protein-membrane interaction with (a) a solid-supported lipid bilayer (SSLB) and (b) small unilamellar vesicles (SUVs). The lipid composition of the membranes as well as the calcium concentrations were varied to investigate lipid specificity and calcium dependency of the binding process. A silicon crystal was used as internal reflection element (IRE) of the ATR cell. Size scales and proportions are not realistic in this illustration.

added to the IRE surface. The vesicle settling onto the IRE was monitored spectroscopically over 40 min at 25 °C. Then the vesicle solution was gently dried for 5 min using a mild N_2 flow. Following this, the procedure was the same as for the bilayer studies: the IRE was rinsed for 20 min using buffer/Ca^{2+} solution to remove unattached vesicles from the supernatant, 65 µl of CaLB protein solution at 0.1 mg/ml concentration were added, and spectra were recorded over a time course of 120 min. Afterwards, the ATR crystal was rinsed with buffer/Ca^{2+} buffer for 40 min. For both, SSLB and vesicle studies, repeated measurements were carried out with new sample preparations to validate the reproducibility.

2.3. ATR-FTIR spectroscopy

Fig. 2 shows the principle of the ATR-FTIR set-up. FTIR spectra were recorded using a Vertex 70v spectrometer and a Bio-ATR II cell (Bruker Optics, Germany). The internal reflection element of the ATR cell consists of a silicon crystal with a refractive index of $n_1 = 3.4$ resulting in a penetration depth of ~0.85 µm at 1000 cm^{-1} for a sample with a refractive index of $n_2 \sim 1.5$ and for an incidence angle of the IR beam of 45°. The ATR unit is a flow-through cell and connected to a peristaltic pump (Ismatec, Switzerland) for controlled inlet and outlet flow of the protein or buffer solution. During the experiments, the flow rate of the peristaltic pump was set at 390 µl/min and the temperature of the ATR cell was maintained at 25 °C using a water bath with an integrated E300 immersion thermostat (LAUDA-Brinkmann, USA). Spectra were recorded with 128 scans and a resolution of 4 cm^{-1}.

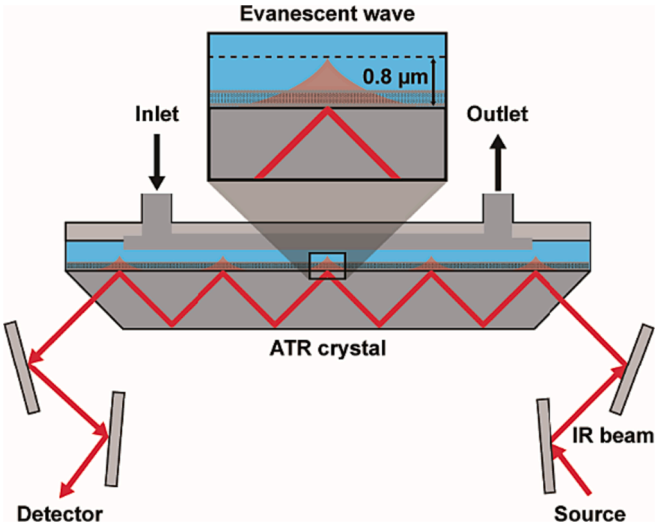

Fig. 2. Schematic representation of the ATR technique with a closed flow system allowing the exchange of solutions without opening the sample chamber. An ATR crystal is the internal reflection element (IRE) and the IR beam is multi-reflected at the IRE surface. The sample sketched here consists of a solid-supported lipid bilayer membrane placed on the IRE surface and the protein solution or buffer in the supernatant (blue). The sample is measured in the evanescent field of the IR beam with a penetration depth of ca. 0.85 µm at 1000 cm^{-1} and for a silicon IRE.

2.4. Spectral analysis

CaLB binding to the membrane was monitored in the IR spectra by the increase in the amide I and amide II bands (protein backbone vibrations) after adding the protein solution to the membrane. Time-dependent spectra were recorded over a time course of 120 min. For quantitative analysis of protein-membrane binding, the amide II band was chosen because it is not interfered by a water band (OH bending vibration). Amide II band areas were integrated between 1600 cm^{-1} and 1500 cm^{-1} for each recorded spectrum using MatLab software (Mathworks, USA). The derived values were plotted over time.

Secondary structure analysis was performed by band deconvolution of the amide I band between 1700 cm^{-1} and 1600 cm^{-1} using OPUS (Bruker Optics, Germany) and OriginPro 2019 software. The number of amide I components and their peak positions were determined by the minima in the second derivative of the amide I spectrum. Curve fitting was performed with a linear combination of Lorentzian and Gaussian band profiles. Peak positions were fixed in accordance to the second derivatives. Bandwidths and intensities were fitted without restriction and by using the Levenberg-Marquardt algorithm. The amide I components correspond to secondary structure elements. The relative amount of each secondary structure was calculated from the integrated area of the corresponding amide I component.

3. Results and discussion

3.1. Protein-membrane binding studies

The binding of CaLB to membranes was studied using ATR-FTIR spectroscopy. Biomimetic membranes were prepared as small lamellar lipid vesicles (SUVs) or as a solid-supported lipid bilayer (SSLB) on the IRE surface of the ATR cell. The different membrane assays were used to analyse if the membrane curvature affects the binding affinity. In order to investigate if CaLB preferentially binds to the inositol phosphate lipid PI(3)P, membranes were composed of either pure POPC lipids or a POPC/PI(3)P (99:1) lipid mixture. The formation of the membrane on the IRE surface was monitored by IR spectra and is shown for a solid-supported lipid bilayer of a POPC/PI(3)P membrane in Fig. 3a. The positive bands occur from functional groups of the lipids. These are the antisymmetric (2923 cm^{-1}) and symmetric (2853 cm^{-1}) stretching vibrations as well as the antisymmetic bending vibration (1466 cm^{-1}) of the CH_2 groups of the alkyl chains, the ester carbonyl stretching vibration (1735 cm^{-1}), and the antisymmetric (1230 cm^{-1}) and symmetric (1087 cm^{-1}) stretching vibrations of the phosphate head groups [12,15]. The negative bands at ~3320 cm^{-1} and ~1640 cm^{-1} result from the water which is displaced when the membrane forms on the IRE surface. The IR spectra indicate that the bilayer formation is complete when the intensities of the lipid bands do not increase further. After the membrane was formed on the IRE surface, the protein solution was added. CaLB binding to the membrane was monitored over time by the increase of the amide I and amide II bands, shown in Fig. 3b. After 120 min, the intensities of the amide bands saturated. Rinsing with buffer had only a marginally effect on the amide intensities and thus verified that the protein was tightly bound to the membrane, and not that the protein just sedimented onto the surface.

Both amide bands are caused by protein backbone vibrations, the amide I (1600–1700 cm^{-1}) is mainly the C═O stretching and the amide II (1600–1500 cm^{-1}) a combination of CN stretching and NH bending vibrations of the peptide groups [10,16]. The amide I band is the commonly used IR marker band for secondary structure analysis. The band can be decomposed into its components which correspond to different secondary structure elements. By analysing the amide I band before and after protein binding, conformational changes can be identified that might occur upon binding to the membrane. The amide II band was chosen for quantitative determination and comparison of the protein binding to different membranes (SSLB, SUV) and at different calcium concentrations because it is not overlayed by the O–H bending vibration of the water at ~1640 cm^{-1} as it is the case for the amide I band. When the protein binds to the membrane, water molecules are displaced from the membrane surface. Thus the binding process causes a decreasing intensity of the water band. The water band interferes with the amide I region so that the intensity of the amide I band is also affected by the change of the water band. The effect is small, but that's why the amide II band was used to quantify the amount of bound protein

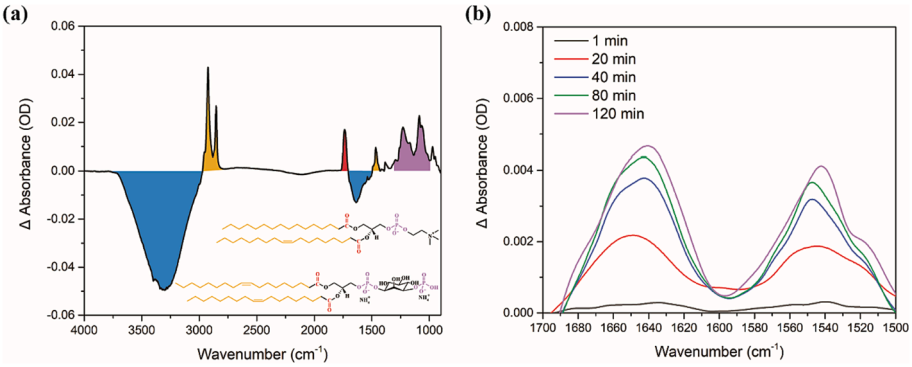

Fig. 3. CaLB binding to a solid-supported POPC/PI(3)P (99:1) lipid bilayer in presence of 20 μM Ca^{2+} (a) Formation of the solid-supported lipid bilayer. Water is displaced from the IRE surface (negative bands, in blue) as the lipid bilayer forms (positive bands). The functional groups of the lipids and corresponding bands are colour coded, yellow for alkyl, red for carbonyl and purple for phosphate groups. (b) The increase of the amide I and amide II band intensities reflects the CaLB binding to the membrane.

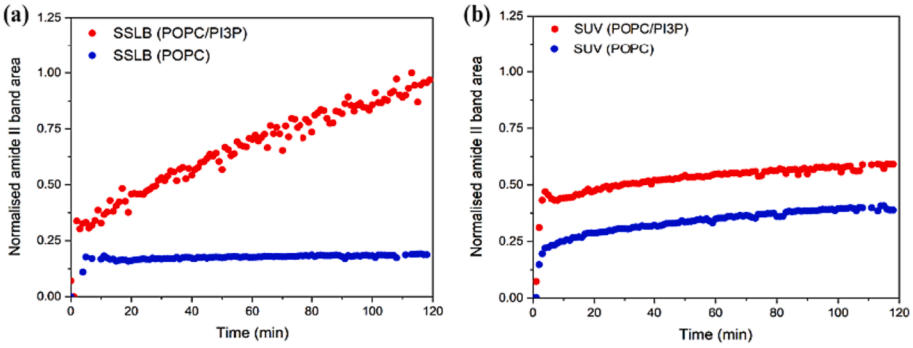

Fig. 4. CaLB binding at 20 μM Ca^{2+} concentration to POPC/PI(3)P (99:1) and to pure POPC (a) solid-supported lipid bilayer (SSLB) and (b) small unilamellar vesicles (SUV). The presence of PI(3)P increases the binding affinity significantly for both, SSLB and SUV. The integrated amide II band areas at 120 min were normalised to SSLB (POPC/PI(3)P).

at different times. The amide II band area was integrated for all recorded spectra and the values were plotted versus time (Fig. 4). The saturated value after 120 min was used as a measure for protein affinity (in arbitrary units).

3.2. Membrane specificity and curvature studies

Fig. 4 compares the binding affinity of CaLB to membranes of pure POPC with mixtures of POPC/PI(3)P in a ratio 99:1. CaLB binds to both membranes, but it becomes obvious that only 1% of the phosphoinositide increases the binding of CaLB significantly. Phosphoinositides have been described as targets for several C2 domains [4,6–9]. The IR measurements support this observation as CaLB shows a specific interaction to PI(3)P. In the measurements with the plain SSLBs (Fig. 4a), the effect is most prominent. For the POPC SSLB, the maximum binding is reached after 5 min whereas further increase is recorded for the POPC/PI(3)P SSLB reaching the maximum value not until 120 min. The binding affinity is increased about a factor of five when PI(3)P is present in the SSLB membrane. An increase in binding affinity is also monitored for the vesicle measurements (Fig. 4b), but the effect is less pronounced as the binding affinity is increased only about a factor of two. One possible reason is that the vesicles form multilayers on the IRE surface reducing the membrane's accessibility for CaLB. Multilayers will also result in a decrease of the amide II band intensity when the protein is further away from the IRE surface as there is an exponential decay of the IR evanescent field detection. In contrast, the preparation of the SSLB leads to the formation of a monolayer [20] with high surface accessibility for protein binding and small distance of the protein from the IRE surface. However, when pure POPC membranes are compared, there is a slightly higher level of CaLB binding to SUVs than to SSLBs. The reasoning for this is not entirely clear. A comparison of the SSLB and SUV spectra are given in in Fig. S1 (Supporting Information, SI). It shows that the SSLB is the more stable and appropriate membrane assay for quantitative ATR-FTIR spectroscopic binding studies. For the SUVs, spectral perturbations occur. Protein and calcium binding change the surface electrostatics and membrane asymmetry and thus can induce rupture or fusion of the SUVs which are under considerable tension, whereas the SSLB is stabilized by the solid support. In summary, our IR studies demonstrate that CaLB binds to plain and curved membranes and that for both membranes a binding specificity is observed for PI(3)P.

3.3. Calcium dependency of CaLB - membrane binding

Calcium has been reported to bind to C2 domain proteins and to be potentially involved in the membrane targeting and binding process. The here studied CaLB protein has not been analysed before with respect to calcium dependencies of protein-membrane binding. For a calcium concentration study, we chose the POPC/PI(3)P SSLB membrane and performed the protein binding experiments as shown in Fig. 4a with different calcium concentrations. The concentrations were varied in a physiologically relevant range, from nM to μM. Each experiment was repeated several times with freshly prepared membranes to ensure reproducibility. The protein binding was quantified by the integrated amide II band area after 120 min. Fig. 5 shows a bar chart of averaged measurements at 200 nM, 2 μM and 20 μM concentrations. The IR measurements reveal that there is an obvious effect of calcium concentration as a significant increase in the binding of CaLB to PI(3)P membranes is observed at higher calcium concentrations.

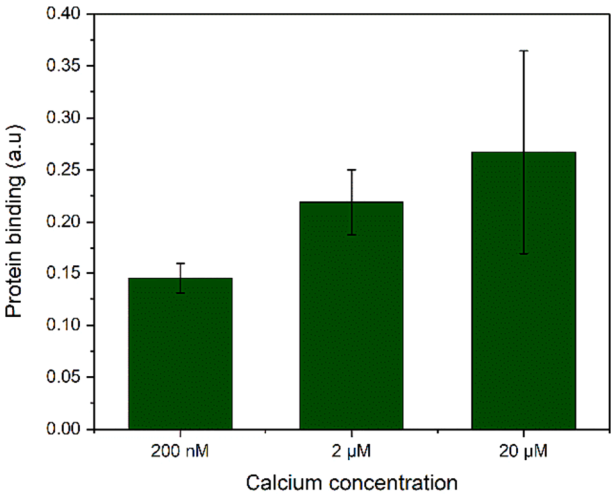

Fig. 5. CaLB binding to a POPC/PI(3)P SSLB membrane (99:1) at varying calcium concentrations. Protein binding was quantified by the integrated amide II band areas. Several repeated measurements were performed at 200 nM, 2 μM, and 20 μM. Protein binding increases with higher calcium concentration in this concentration range.

3.4. Conformational changes upon binding

ATR–FTIR can be applied for the analysis of protein conformation. The amide I region of the IR spectrum between 1600 cm^{-1} and 1700 cm^{-1} contains information of the secondary structure of proteins. The shape of the amide I band indicates the structural composition of the secondary structure elements and band deconvolution reveals an estimation of the individual components. The band deconvolution is done by allocating secondary structure elements to the corresponding amide I component within the amide I band. The peak position of each component was determined from the minima in the second derivative of the spectrum. The area under each fitted curve represents the fraction of the respective structural element.

Fig. 6 depicts the secondary structure analyses of CaLB in solution and CaLB bound to the PI(3)P SSLB membrane (recorded after 120 min). The fitted amide I components were assigned to the secondary structure elements according to their characteristic frequency ranges [10]. The assignment of a given component band to a secondary structure type is not unique or straightforward because secondary structure elements of proteins absorb in frequency ranges which can overlap. This is the case for α-helices and disordered structures, which both absorb in a range between approximately 1640 cm^{-1}–1660 cm^{-1}, α-helices tend to absorb at higher frequencies than disordered structure but there are also other examples [10]. We assigned the fitted component with the higher frequency to α-helices and the lower component to disordered structures.

One should keep in mind that the common fold of C2 domain modules consists of large flexible loops interconnecting the sheets of the β-barrel core, with relatively small α-helical parts [4]. Thus we assume that the component assigned to α-helices contains also the more disordered loop structures. To analyse if conformational changes are induced by the membrane binding, we performed amide I curve fitting for the solution and the bound CaLB structure and compared the relative changes in the components. The fits provided band components for the solution structure (Fig. 6a) with a relative area of 11% for disordered structure at 1645 cm^{-1}, 37% for α-helices at 1660 cm^{-1}, and 52 % for the two components at 1630 and 1680 cm^{-1} representing anti-parallel β-sheets. The spectrum was recorded at the beginning of the experiment, just after addition of the protein, but in presence of the membrane. As a control we measured CaLB in buffer solution without membrane and performed a secondary analysis (Fig. S2, SI) revealing similar results and confirming the conformational composition of the solution structure. In the bound CaLB structure (Fig. 6b), the relative area of the deconvoluted bands for antiparallel β-sheets decreased from 52% to 38%. An increase from 11% to 17% was found for the disordered structure and from 37% to 45% for the α-helical component. Overall, the IR spectra indicate that binding of CaLB is accompanied by minor conformational changes being consistent with what is reported from crystal structural data of C2 domains with lipid molecules [6,26–28].

4. Conclusion

The here presented experimental ATR-FTIR approach is highly suitable to characterize C2 domain proteins and gain molecular insights into their membrane interaction and conformational dynamics. Biomimetic membranes can be prepared with different lipid compositions to explore if C2 domain proteins bind to specific inositol phospholipids. Binding affinities can be quantified and the response of C2 domains to different calcium concentrations further investigated. Protein-protein interactions also play an important role for the regulation of membrane trafficking events. To shed light also on the recruitment process and the interplay of proteins at the membrane, future studies will focus on how protein-protein interactions impact the binding affinity and binding kinetics to the membrane.

CRediT authorship contribution statement

Shane Maguire: Conceptualization, Formal analysis, Investigation, Methodology, Writing - original draft. **Christian Scheibe:** Investigation, Methodology. **Terese Eisgruber:** Investigation, Methodology. **Niccolò Mosesso:** Conceptualization, Investigation, Methodology. **Erika Isono:** Conceptualization, Funding acquisition, Project administration, Supervision, Writing - review & editing. **Karin Hauser:** Conceptualization, Funding acquisition, Project administration, Supervision, Writing - original draft, Writing - review & editing.

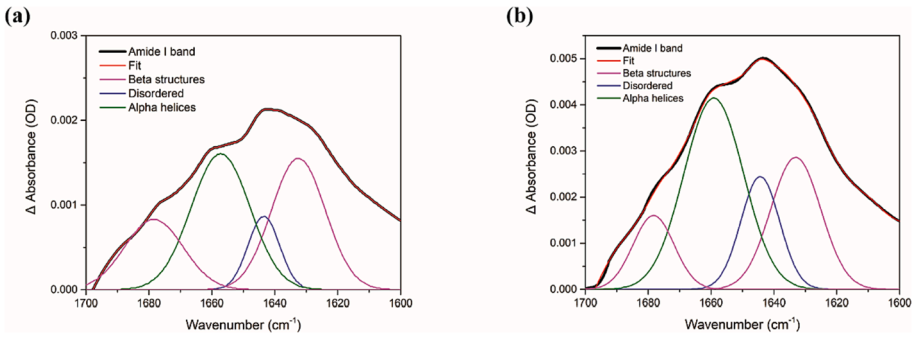

Fig. 6. Conformational changes of CaLB occurring upon binding to a POPC/PI(3)P SSLB membrane (99:1) at 20 μM Ca^{2+} concentration. Secondary structure analysis by spectral deconvolution of the amide I band reveals a slight increase of α-helical and disordered structures relative to the β-sheets. Structural composition of (a) CaLB in solution (b) CaLB bound to the POPC/PI(3)P membrane.

Declaration of Competing Interest

The authors declare that they have no known competing financial interests or personal relationships that could have appeared to influence the work reported in this paper.

Data availability

Data will be made available on request.

Acknowledgments

Financial support by the Deutsche Forschungsgemeinschaft (SFB 969, A02 to K.H. and C08 to E.I.) is gratefully acknowledged. We appreciate the support of D. Alonso Cerrón-Infantes with the graphical designs.

Appendix A. Supplementary data

Supplementary data to this article can be found online at https://doi.org/10.1016/j.saa.2023.123629.

References

[1] E.A. Nalefski, J.J. Falke, The C2 domain calcium-binding motif: structural and functional diversity, Protein Sci. 5 (1996) 2375–2390.
[2] S. Corbalan-Garcia, J.C. Gomez-Fernandez, Protein kinase C regulatory domains: the art of decoding many different signals in membranes, BBA 1761 (2006) 633–654.
[3] W. Cho, R.V. Stahelin, Membrane binding and subcellular targeting of C2 domains, BBA 1761 (2006) 838–849.
[4] S. Corbalan-Garcia, J.C. Gomez-Fernandez, Signaling through C2 domains: more than one lipid target, BBA 2014 (1838) 1536–1547.
[5] G. Di Paolo, P. De Camilli, Phosphoinositides in cell regulation and membrane dynamics, Nature 443 (2006) 651–657.
[6] S.H. Chung, W.J. Song, K. Kim, J.J. Bednarski, J. Chen, G.D. Prestwich, R.W. Holz, The C2 domains of Rabphilin3A specifically bind phosphatidylinositol 4,5-bisphosphate containing vesicles in a Ca2+-dependent manner. In vitro characteristics and possible significance, J. Biol. Chem. 273 (1998) 10240–10248.
[7] S. Corbalan-Garcia, J. Garcia-Garcia, J.A. Rodriguez-Alfaro, J.C. Gomez-Fernandez, A new phosphatidylinositol 4,5-bisphosphate-binding site located in the C2 domain of protein kinase Calpha, J. Biol. Chem. 278 (2003) 4972–4980.
[8] G. Schiavo, Q.-M. Gu, G.D. Prestwich, T.H. Söllner, J.E. Rothman, Calcium-dependent switching of the specificity of phosphoinositide binding to synaptotagmin, PNAS 93 (1996) 13327–13332.
[9] R.B. Jensen, K. Lykke-Andersen, G.I. Frandsen, H.B. Nielsen, J. Haselhoff, H. M. Jespersen, J. Mundy, K. Skriver, Promiscuous and specific phospholipid binding by domains in ZAC, a membrane-associated *Arabidopsis* protein with an ARF GAP zinc finger and a C2 domain, Plant Mol. Biol. 44 (2000) 799–814.
[10] A. Barth, C. Zscherp, What vibrations tell us about proteins, Q. Rev. Biophys. 35 (2002) 369–430.
[11] E. Goormaghtigh, V. Raussens, J.-M. Ruysschaert, Attenuated total reflection infrared spectroscopy of proteins and lipids in biological membranes, BBA 1422 (1999) 105–185.
[12] L.K. Tamm, S.A. Tatulian, Infrared spectroscopy of proteins and peptides in lipid bilayers, Q. Rev. Biophys. 30 (1997) 365–429.
[13] R.N. Lewis, R.N. McElhaney, Membrane lipid phase transitions and phase organization studied by Fourier transform infrared spectroscopy, BBA 2013 (1828) 2347–2358.
[14] J. Mihaly, R. Deak, I.C. Szigyarto, A. Bota, T. Beke-Somfai, Z. Varga, Characterization of extracellular vesicles by IR spectroscopy: Fast and simple classification based on amide and CH stretching vibrations, Biochim. Biophys. Acta Biomembr. 2017 (1859) 459–466.
[15] S.A. Tatulian, Attenuated Total Reflection Fourier Transform Infrared Spectroscopy: A Method of Choice for Studying Membrane Proteins and Lipids, Biochemistry 42 (2003) 11898–11907.
[16] H. Yang, S. Yang, J. Kong, A. Dong, S. Yu, Obtaining information about protein secondary structures in aqueous solution using Fourier transform IR spectroscopy, Nat. Protoc. 10 (2015) 382–396.
[17] G.B. Berselli, N.K. Sarangi, S. Ramadurai, P.V. Murphy, T.E. Keyes, Microcavity-Supported Lipid Membranes: Versatile Platforms for Building Asymmetric Lipid Bilayers and for Protein Recognition, ACS Appl. Bio Mater. 2 (2019) 3404–3417.
[18] C. Bolterauer, H. Heller, Calculation of IR dichroic values and order parameters from molecular dynamics simulations and their application to structure determination of lipid bilayers, Eur. Biophys. J. 24 (1996) 322–334.
[19] M.A. Fallah, H.R. Gerding, C. Scheibe, M. Drescher, C. Karreman, S. Schildknecht, M. Leist, K. Hauser, Simultaneous IR-Spectroscopic Observation of alpha-Synuclein, Lipids, and Solvent Reveals an Alternative Membrane-Induced Oligomerization Pathway, Chembiochem 18 (2017) 2312–2316.
[20] C. Kötting, J. Güldenhaupt, K. Gerwert, Time-resolved FTIR spectroscopy for monitoring protein dynamics exemplified by functional studies of Ras protein bound to a lipid bilayer, Chem. Phys. 396 (2012) 72–83.
[21] P. Pinkerneil, J. Guldenhaupt, K. Gerwert, C. Kotting, Surface-attached polyhistidine-tag proteins characterized by FTIR difference spectroscopy, ChemPhysChem 13 (2012) 2649–2653.
[22] C. Scheibe, K. Hauser, Orientation of lipids in solid supported lipid bilayers studied by polarized ATR-FTIR spectroscopy1, Biomed. Spectrosc. Imaging 7 (2018) 17–24.
[23] C. Scheibe, C. Karreman, S. Schildknecht, M. Leist, K. Hauser, Synuclein Family Members Prevent Membrane Damage by Counteracting alpha-Synuclein Aggregation, Biomolecules 11 (2021).
[24] M.L. Wagner, L.K. Tamm, Tethered Polymer-Supported Planar Lipid Bilayers for Reconstitution of Integral Membrane Proteins: Silane-Polyethyleneglycol-Lipid as a Cushion and Covalent Linker, Biophys. J. 79 (2000) 1400–1414.
[25] R. Mendelsohn, G. Mao, C.R. Flach, Infrared reflection-absorption spectroscopy: principles and applications to lipid-protein interaction in Langmuir films, BBA 1798 (2010) 788–800.
[26] M. Guerrero-Valero, C. Ferrer-Orta, J.-M.-V. Querol-Audi, C.I. Fita, J.C. Gomez-Fernandez, N. Verdaguer, S. Corbalan-Garcia, Structural and mechanistic insights into the association of PKCa-C2 domain to PtdIns(4,5)P2, PNAS 106 (2009) 6603–6607.
[27] J. Guillen, C. Ferrer-Orta, M. Buxaderas, D. Perez-Sanchez, M. Guerrero-Valero, G. Luengo-Gil, J. Pous, P. Guerra, J.C. Gomez-Fernandez, N. Verdaguer, S. Corbalan-Garcia, Structural insights into the Ca2+ and PI(4,5)P2 binding modes of the C2 domains of rabphilin 3A and synaptotagmin 1, PNAS 110 (2013) 20503–20508.
[28] Y. Hirano, Y.G. Gao, D.J. Stephenson, N.T. Vu, L. Malinina, D.K. Simanshu, C. E. Chalfant, D.J. Patel, R.E. Brown, Structural basis of phosphatidylcholine recognition by the C2-domain of cytosolic phospholipase A(2)alpha, Elife 8 (2019).